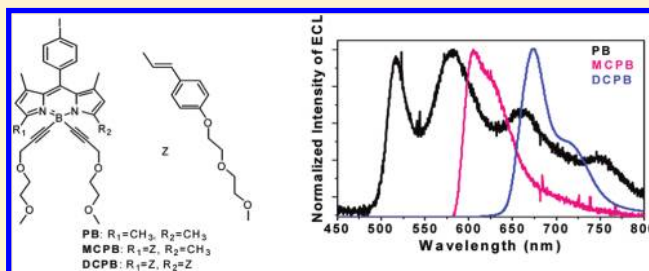


Electrochemistry and Electrogenerated Chemiluminescence of Some BODIPY Derivatives

Jungdon Suk,[†] Khalid M. Omer,[†] Thomas Bura,[‡] Raymond Ziessel,[‡] and Allen J. Bard^{*†}[†]Center for Electrochemistry and Department of Chemistry and Biochemistry, The University of Texas at Austin, Austin, Texas 78712, United States[‡]Laboratoire de Chimie Moléculaire et Spectroscopies Avancées (LCOSA), UMR 7515, Ecole Européenne de Chimie, Polymères et Matériaux (ECPM), CNRS, 25 rue Becquerel, 67087 Strasbourg Cedex 02, France**S** Supporting Information

ABSTRACT: The electrochemistry, spectroscopy, and electrogenerated chemiluminescence (ECL) of three BODIPY derivatives, PB, MCPB, and DCPB, are investigated. Cyclic voltammetry of all three derivatives shows at low scan rates reversible reduction waves and less reversible oxidation waves (consistent with lack of substitution in the 2 and 6 positions). The three compounds are highly fluorescent in MeCN emitting in the green to the red regions. All of the three compounds produce intense ECL, strong enough to be seen with the naked eye in a lighted room, but are not stable under continued pulsing of potential because of instability of the radical cation, ultimately producing an insulating polymer layer on the electrode surface. The ECL spectra are at essentially the same wavelengths as the photoluminescence (PL) spectra for MCPB and DCPB, assigned as emission by the T- or ST-route. The ECL spectra of PB show four peaks at 516, 581, 663, and 752 nm. The peaks at 581, 663, and 752 nm are not present in the PL spectrum. The first ECL peak is attributed to the singlet excited state at essentially the same wavelength as PL, while oligomers or other byproducts are probably responsible for the additional two ECL peaks (581 and 663 nm) based on the results from bulk electrolysis and mass spectroscopy.



INTRODUCTION

We report the electrochemical, photophysical characterization and electrogenerated chemiluminescence (ECL) of three derivatives of borodipyrromethene (BODIPY) moieties.

4,4'-Difluoro-4-bora-3a,4a-diaza-5-indacene is abbreviated as BODIPY; Figure 1a shows the basic structure and numbering scheme of the BODIPY framework. While most studies of BODIPY dyes involve the 4,4' positions being fluorinated, non-fluorinated BODIPY dyes can lead to a wider range of molecular properties, depending on the nature of the 4,4'-substituents.

After the first report by Treibs and Kreuzer in 1968,¹ BODIPY-based compounds have increased in popularity because of their excellent thermal and photochemical stabilities, high fluorescence quantum yields, high absorbances, good solubilities, and chemical robustness.² Several derivatives of BODIPY have been developed and studied, and the ability to tune their photophysical properties has increased their potential applications as labels in biological studies,³ organic light emitting diodes,⁴ laser dyes,⁵ light-harvesters,⁶ and sensitizers for solar cells.⁷ The various types of substituents attached to any of the available sites in BODIPY can affect the emission wavelength, the redox potentials, and the stability of the electrogenerated radical ions. Most studies of BODIPY-based compounds have focused on their photophysical properties.⁸ However, a number of functionalized BODIPY dyes

have been used for electrogenerated chemiluminescence (ECL) generated by alternating the potential to generate radical anions and cations that annihilate to form an emitting state. Electrochemical studies show that, in general, BODIPY dyes that are unsubstituted in positions 2 and 6 tend to show irreversible voltammetric waves for the oxidation, because of instability of radical cations, leading to poor ECL behavior.⁹ Lack of substitutions in the other positions, especially 8, leads to instability of the radical anions. Therefore, tailoring the molecular structure via appropriate substitutions on the BODIPY is a key factor in tuning the electrochemical and photophysical properties. It is desirable in ECL to have stable and long-lived radical ions with apparent high PL quantum yield to obtain strong and bright ECL. Developing such highly efficient and stable ECL emitters over a broad spectrum of wavelength has been of interest for many years and might find application as an ECL label for analytical purposes, for example, for DNA determination and immunoassay.¹⁰

ECL is a type of luminescence that involves the generation of oxidized and reduced species, often radical ions, at electrode surfaces that undergo a fast electron transfer reaction to produce

Received: February 24, 2011

Revised: June 30, 2011

Published: June 30, 2011

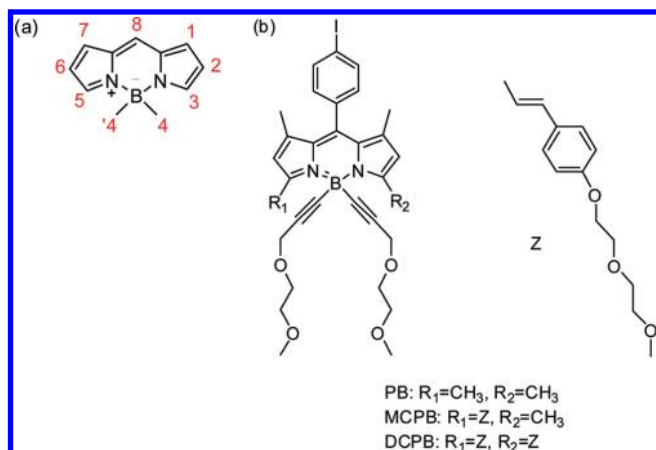
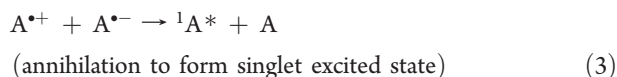
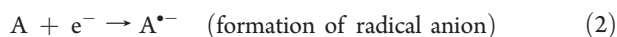
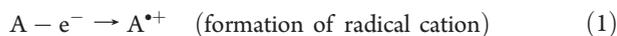
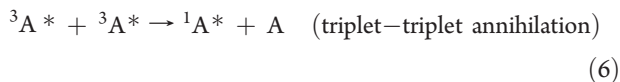
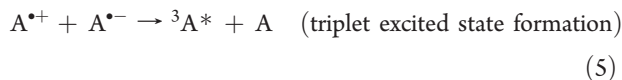


Figure 1. (a) Numbering scheme used for the BODIPY framework. (b) Structures of BODIPY-based molecules: PB, MCPB, and DCPB.

an excited state.^{11,12} This radical ion annihilation reaction sequence can be represented as



This pathway is called S-route ECL or an “energy sufficient system”, that is, the annihilation energy is sufficient to populate the excited singlet state. Many ECL reactions of this type have been studied and their mechanisms are well understood. If the energy is not sufficient to populate the singlet state, triplet–triplet annihilation can occur. This is called the T-route or an “energy deficient system”.



We show in this paper the electrochemistry, photophysics, and ECL of a series of BODIPY derivatives. The electrochemical reduction, oxidation, and radical ion annihilation of ECL of these BODIPY derivatives are described below. Photophysical measurements were carried out and a comparison of their ECL spectra with PL is discussed.

EXPERIMENTAL SECTION

Chemicals. PB, MCPB, and DCPB, whose structures are shown in Figure 1b, were synthesized in two steps from 8-(4-iodophenyl)-1,3,5,7-tetramethyl-4,4-difluoro-4-bora-3a,4a-diazas-indacene.¹³ All three have 1,7 = Me, 2,6 = H, 4,4' = R₁ = C≡CCH₂OCH₂CH₂OCH₃, and 8 = *p*-iodophenyl; the molecules of interest are PB (3,5 = Me), MCPB (3 = Me, 5 = R₂),

and DCPB (3,5 = R₂), where R₂ is CH=CH-Ph-O-(CH₂CH₂O)₂CH₃. Anhydrous acetonitrile (MeCN, 99.93%) was obtained from Aldrich (St. Louis, MO). Tetra-*n*-butylammonium hexafluorophosphate (TBAPF₆) was obtained from Fluka and used as received. All solutions were prepared in a He atmosphere glovebox (Vacuum Atmospheres Corp. Hawthorne, CA) and placed in an airtight cell for measurements completed outside of the box.

Characterization. The electrochemical cell consisted of a Pt wire counterelectrode (CE), an Ag wire quasi-reference electrode (QRE) and a 2 mm diameter Pt disk inlaid in glass working electrode (WE). All potentials were calibrated against an SCE by the addition of ferrocene as an internal standard at the end of all measurements, taking $E_{\text{Fc}/\text{Fc}^+}^{\circ} = 0.342 \text{ V vs SCE}$.¹⁴ The working electrode was bent at a 90° angle (J-type electrode) so that the electrode surface faced the detector in ECL experiments. Before each experiment, the working electrode was polished on a felt pad with 1, 0.3, and 0.05 μm alumina (Buehler, Ltd., Lake Bluff, IL) and then sonicated in DI water and ethanol for 1 min each. The electrode was rinsed with acetone, dried in the oven, and transferred into the glovebox. Cyclic voltammograms were obtained on a CH Instruments (Austin, TX) model 660 electrochemical workstation. Digital simulations of cyclic voltammograms were performed using DigiSim 3.03 (Bioanalytical Systems, Inc., West Lafayette, IN).

UV–vis spectra were recorded with a Milton Roy Spectronic 3000 array spectrophotometer. Fluorescence spectra were collected on a QuantaMaster spectrofluorometer (Photon Technology International, Birmingham, NJ). For the ECL spectra, the detector was a liquid nitrogen charge-coupled device (CCD) camera (Princeton Instruments, SPEC-32). The camera was cooled with liquid nitrogen between −100 and −120 °C, and the spectral wavelengths were calibrated with a mercury lamp. Faradaic current and ECL transients were simultaneously recorded by an Autolab electrochemical workstation (Eco Chemie, The Netherlands) coupled with a photomultiplier tube (PMT, Hamamatsu R4220p, Japan) held at −750 V with a high-voltage power supply (Kepco, Flushing, NY). ECL transients were generated by pulsing the electrode 80 mV beyond the diffusion-limited peak potentials for the oxidation and reduction peaks.

Bulk electrolysis was performed in a three-compartment cell separated by fine porosity glass frits. The WE was a Pt mesh electrode (surface area: 4.8 cm²), the CE was a Pt wire, and the RE was an Ag/AgNO₃ (0.1 M) electrode in MeCN with a porous Vycor tip separator. The WE and RE were placed in the first compartment with 4 mL of 1 mM PB and 0.1 M TBAPF₆ in MeCN. A magnetic stirring bar was used to maintain uniform analyte concentration in the solution. The second compartment and the third compartment that held the CE contained 0.1 M TBAPF₆ in MeCN. The potential was controlled at $E_{\text{p,red}} - 100 \text{ mV}$ using the Autolab electrochemical workstation. The solution was electrolyzed until the current became constant and 99.5% of the original amount was electrolyzed.

RESULTS AND DISCUSSION

Electrochemistry. Cyclic voltammetry (CV) was used to obtain information about the electrochemistry of the compounds, to determine the stability of the radical ions in MeCN with 0.1 M TBAPF₆ and to estimate the energy of annihilation in ECL. All three compounds show a nernstian one-electron reduction wave and a less reversible one electron oxidation (Figure 2). The results

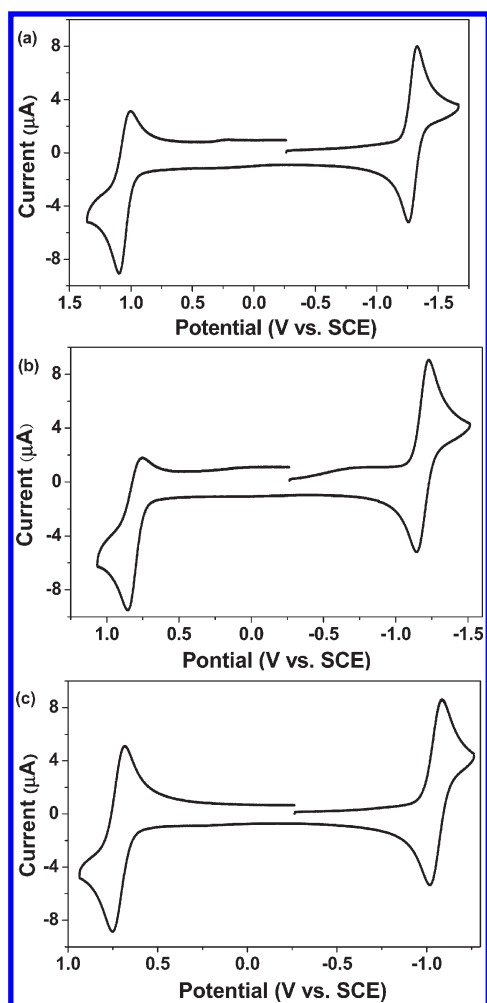


Figure 2. Cyclic voltammogram of 0.5 mM (a) PB, (b) MCPB, (c) DCPB in MeCN with 0.1 M TBAPF₆: WE, Pt disk; CE, Pt coil; RE, Ag wire QRE. Scan rate was 0.5 V/s.

Table 1. Electrochemical Data

chemical	$E_{1/2}$ (V vs SCE)		D (cm ² /s)	E_g^a (eV)	E_{HOMO}^b (eV)	E_{LUMO}^c (eV)
	A/A ⁻	A/A ⁺				
PB	-1.29	1.05	3×10^{-5}	-2.34	-5.81	-3.47
MCPB	-1.18	0.81	2×10^{-5}	-1.99	-5.57	-3.58
DCPB	-1.05	0.72	2×10^{-5}	-1.77	-5.48	-3.71

^a From the CV. ^b The HOMO values are calculated based on the value of -4.8 eV in vacuum for ferrocene. $E_{\text{HOMO}} = -E_{\text{ox}} - 4.8$ eV. ^c From the reduction wave. $E_{\text{LUMO}} = E_g - E_{\text{HOMO}}$. $E_g = E_{\text{ox}} + E_{\text{red}}$.

are summarized in Table 1. The CV of PB at scan rate, ν , of 0.5 V/s showed a voltammetric half-wave potential $E_{1/2} = 1.05$ V versus SCE and chemical irreversibility in the oxidation wave suggesting a following reaction of the radical cation. With higher ν , for example, 1–20 V/s, the wave became reversible. The negative scan showed a nernstian reduction wave at $E_{1/2} = -1.29$ V versus SCE. The peak separation of ~ 70 mV, slightly larger than the expected value for nernstian behavior for one electron transfer reversible peak separation, 59 mV, can be attributed to the high

uncompensated resistance ($R_u \sim 700 \Omega$). Although MCPB is more blocked near the reactive 6 position compared to PB, the oxidation was less chemically reversible at $E_{1/2} = 0.81$ V even as $\nu = 1$ V/s. In this molecule, the 2-position is unblocked and perhaps the substitution in the 5-position increases the positive charge density at 2. Products of a possible oxidative polymerization have not been identified, but some studies suggest that these byproducts could be analogous to polypyrrole.¹⁵ The negative scan showed a reversible reduction wave at $E_{1/2} = -1.18$ V versus SCE.

However, DCPB, the most highly blocked of the three, showed chemically reversible, nernstian oxidation, and reduction waves at $E_{1/2} = 0.72$ V and -1.05 V versus SCE, respectively, at all ν , indicating stability of the radical ions on the time scale of the experiment. The bulky substituent groups on the 3 and 5 positions block the 2 and 6 positions preventing dimerization or other reactions (e.g., deprotonation by trace base). Compared with the other two compounds, DCPB is more easily oxidized and reduced probably because the greater π -conjugation reduces the HOMO–LUMO energy gap (estimated from the difference in the first oxidation and reduction wave potentials). The peak current ratio ($i_{\text{pa}}/i_{\text{pc}}$) of the reduction wave of the three compounds was approximately unity, indicating the absence of following chemical reactions and good stability of the radical ions. Moreover, scan rate studies showed that the peak current of the reduction wave was proportional to the square root of the scan rate ($\nu^{1/2}$; Supporting Information, Figure S1).

Digital simulation of cyclic voltammogram at different scan rates helped to obtain information about possible mechanisms of electrode reactions. The uncompensated resistance and capacitance were obtained by performing a potential step in the system at potentials where no faradaic reactions occur (0.4 V vs SCE). Figures 3 and Supporting Information, Figure S2 show the simulation of both oxidation and reduction of PB at different scan rates from 50 mV/s to 20 V/s. The oxidation CVs could be fit to an $E_r C_r$ mechanism, a chemical reaction following an electrochemical electron transfer, with a homogeneous forward rate constant, $k_f = 2.7 \times 10^4 \text{ s}^{-1}$, $K_{\text{eq}} = 410$ and a heterogeneous rate constant, $k^\circ = 0.07$ cm/s. For the reduction of PB, an $E_r C_r$ mechanism is also followed, with a much slower homogeneous forward reaction, $k_f = 0.1 \text{ s}^{-1}$, $K_{\text{eq}} = 10$ with a heterogeneous rate constant, $k^\circ = 0.036$ cm/s. For the oxidation of MCPB, the simulation showed an $E_r C_r$ mechanism, with $k_f = 2 \text{ s}^{-1}$, $K_{\text{eq}} = 15$, and a heterogeneous rate constant, $k^\circ = 0.1$ cm/s (Supporting Information, Figure S3). However, both oxidation and reduction of DCPB and the reduction wave of MCPB were nernstian at all scan rates investigated (Supporting Information, Figures S4–S6). Some information about the nature of the products of the homogeneous following reactions, especially PB, was obtained from bulk electrolysis experiments followed and mass spectrometric examination of the solution and from the ECL response. These are discussed in the section on bulk electrolysis.

Upon scanning to more extreme potentials in both the negative and the positive directions, additional waves were observed (Figure 4). In all cases they were chemically irreversible, showing that the dianions and dications undergo very rapid following reactions. Thus, the potentials at which second waves occur (Table 1) are at less extreme potentials than their nernstian (thermodynamic) standard potentials. Even with the rapid following reactions, the spacing between the first and second waves is large, 1 V for the reduction and 400 mV for oxidation. As shown elsewhere,¹⁶ BODIPY compounds show anomalously large splitting compared to aromatic hydrocarbons¹⁷ and other heterocyclic

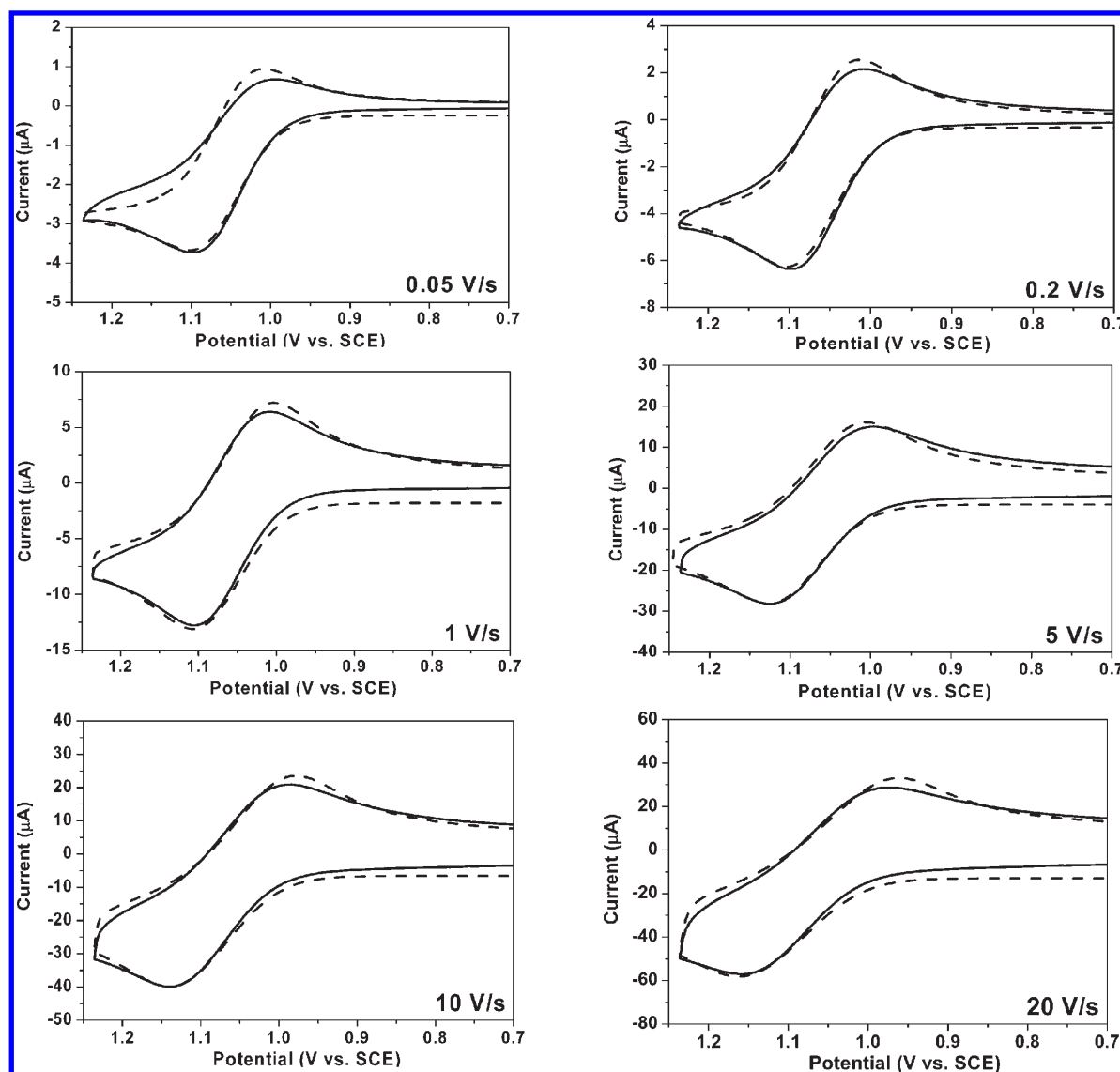


Figure 3. Simulation of oxidation of 0.5 mM PB compared to experimental CVs. The simulation is corrected for resistance (700Ω) and capacitance ($100 \mu\text{F}$): $k_f = 2.7 \times 10^4$, $K_{\text{eq}} = 410$. Experimental (solid line), simulation (dotted line). $k^{\circ} = 0.07 \text{ cm/s}$, $\alpha = 0.5$, $D = 3 \times 10^{-5} \text{ cm}^2/\text{s}$.

compounds. The PB compound did not show clear second waves on oxidation. The presence of oxidizable cinnamyl groups in positions 3 and 5 causes additional peaks to appear because of the oxidation of these substituents, before the second oxidation of the BODIPY nucleus. Thus, the peak current ratio between the first and the second oxidation wave of MCPB is about 1, indicating the only source of the secondary oxidation is the presence of one cinnamyl group. However, the peak current ratio between the first and the second oxidation wave of DCPB is about 2, consistent with the second oxidation wave being caused by two cinnamyl groups that oxidize at essentially the same potential (i.e., no interaction between the cinnamyl groups; Supporting Information, Figure S7).

Spectroscopy. Spectroscopic experiments were performed for all of the compounds in the same solvent as that used for the electrochemical measurements. The absorbance and photoluminescence of these compounds are shown in Figure 5 and the data are summarized in Table 2. The UV–vis spectra show sharp absorption peaks at 497 nm (PB), 568 nm (MCPB), and 641 nm (DCPB), with the shift to longer wavelengths confirming the

effects of increasing delocalization for the position 3 and 5 cinnamyl substituents. The PL spectra of these compounds feature a single intense peak that is the mirror image of the absorbance spectrum with λ_{max} at 506 nm (PB), 579 nm (MCPB), and 655 nm (DCPB). The sharp absorption and fluorescence maxima (20–30 nm), high extinction coefficients, and high fluorescence quantum yields (>0.5) are features for BODIPY derivatives. The addition of the oligo-oxyethylene chains and cinnamyl groups, leads to shifts in the absorption and fluorescence maxima to longer wavelengths probably because of extension of π -conjugation, i.e., additional π -conjugation reduces the energy gap of lowest π to π^* transition. Each oligo-oxyethylene chain and cinnamyl group cause a spectral shift in MeCN of ~ 70 nm in the absorption and ~ 73 nm in the fluorescence bands. This trend is also reflected in the decreasing potential differences in the potentials of the first oxidation and reduction waves.

As shown in Table 2, all three compounds show a relatively small Stokes shift, consistent with molecular rigidity and little reorganization on excitation and emission in these dyes. A gradual

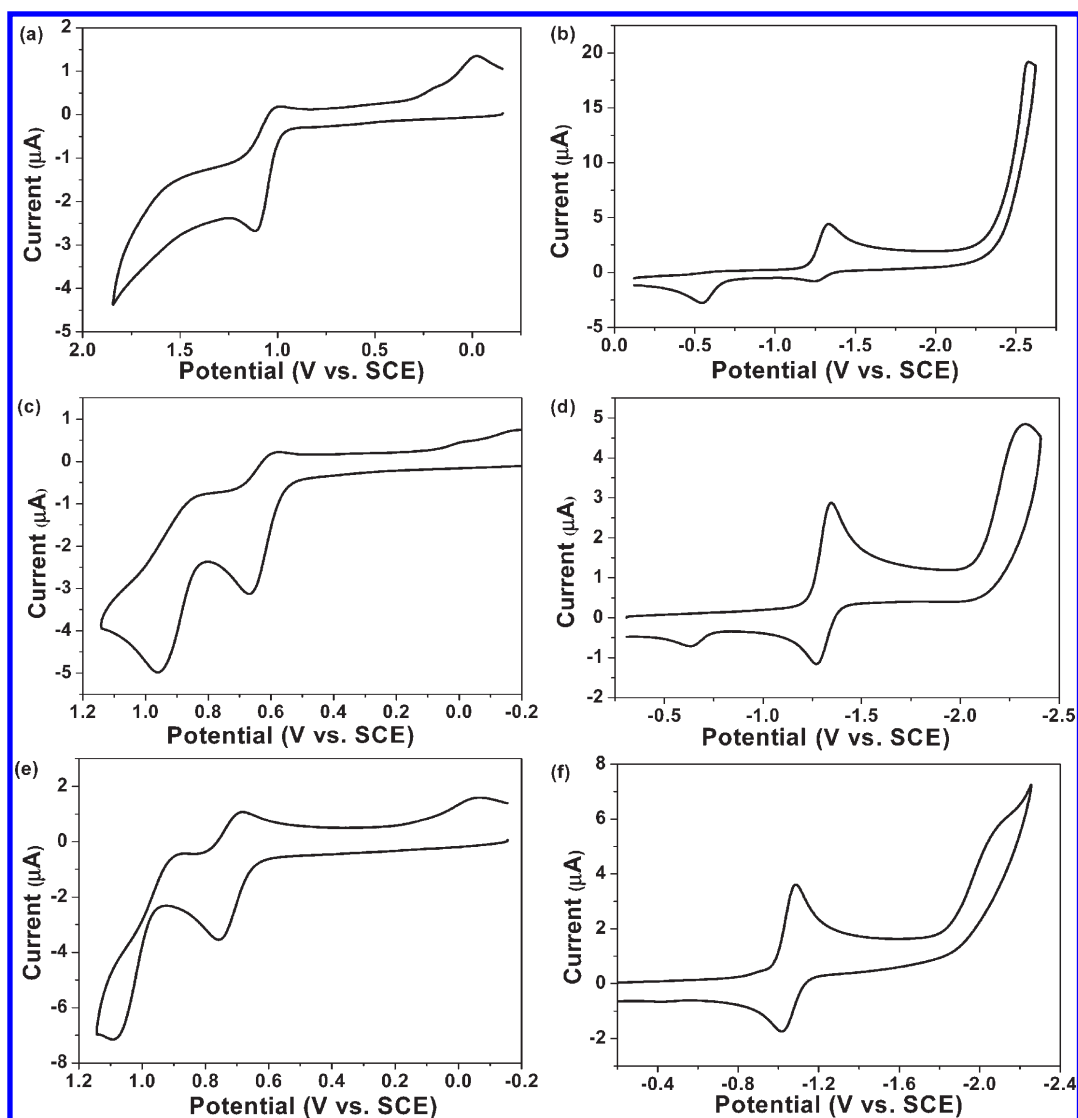


Figure 4. Cyclic voltammograms of 0.5 mM (a, b) PB, (c, d) MCPB, (e, f) DCPB in MeCN with 0.1 M TBAPF₆. WE: Pt disk, CE: Pt coil, RE: Ag wire as a QRE. Scan rate was 0.2 V/s: (a, c, e) anodic scans; (b, d, f) cathodic scans.

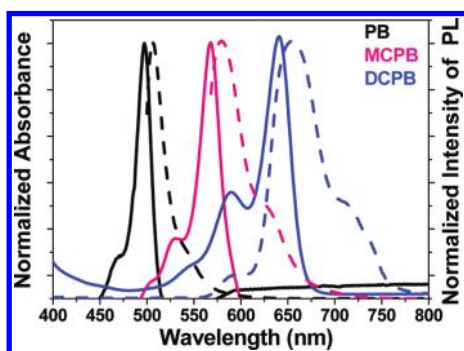


Figure 5. Absorbance spectra (solid lines) and fluorescence spectra (dashed lines) of BODIPY compounds, PB (black), MCPB (pink), and DCPB (blue), in MeCN with 0.1 M TBAPF₆. Emission spectra were excited at the absorption maxima.

increase in the Stokes shift is generally observed with an increasing extent of substitution owing to changes in the molecular structure of compounds upon the excitation.¹⁸

Electrogenerated Chemiluminescence (ECL). Figure 6 shows the ECL spectra of the three BODIPY compounds in MeCN with 0.1 M TBAPF₆ during repeated pulsing (pulse width = 0.1 s) between potentials where oxidized and reduced forms were alternately produced (with a 3 min integration time). All compounds produced ECL emission visible with the naked eye in a dark room. Many BODIPY compounds show strong ECL emission because of the good stability of the radical cations and anions in solution.⁹ However, the ECL intensity of the compounds, except for DCPB, decreased to nondetectable levels after 6000 s of pulsing, while a film forms on the surface of the working electrode. This is probably a polymer formed by anodic electropolymerization, as found with pyrroles and oligofluorenes.¹⁹ To confirm that the film on the surface of the electrode blocks faradaic reactions, the cell was returned to the glovebox. When the electrode was polished, emission of ECL and electrochemistry were restored again with repeated pulsing.

The ECL emission of DCPB corresponded quite closely to the PL spectrum. A small red shift in the ECL spectrum is probably caused by an inner-filter effect because of the difference of

Table 2. Spectroscopic and ECL Data

chemical	$\lambda_{\max(\text{abs})}$ (nm)	$\lambda_{\max(\text{PL})}$ (nm)	Φ_{PL}^a	$\lambda_{\max(\text{ECL})}$ (nm)	Φ_{ECL}^b	$-\Delta G_{\text{ann}}^c$ (eV)	$-\Delta H_{\text{ann}}^d$ (eV)	E_s^e (eV)
PB	497	506	0.64	516, 581, 663, 752	0.04	2.34	2.24	2.45
MCPB	568	579	0.71	605	0.03	1.99	1.89	2.14
DCPB	641	655	0.28	674	~1	1.77	1.67	1.89

^a Φ_{PL} is the relative PL compared to DPA. $\Phi_{\text{PL, DPA}} = 0.91$ in benzene. ^b Φ_{ECL} is the relative ECL compared to DPA. $\Phi_{\text{ECL, DPA}} = 1$. ^c $-\Delta G_{\text{ann}} = E_{\text{pa}}^{\text{ox}} - E_{\text{pc}}^{\text{red}}$. ^d $-\Delta H_{\text{ann}} = -\Delta G_{\text{ann}} - 0.1$. ^e $E_s = 1239.85/\lambda_{\max}^{\text{PL}}$ (nm).

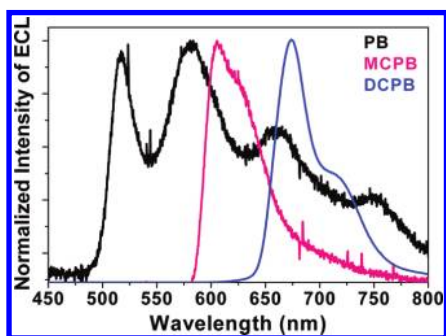


Figure 6. ECL spectra of PB (black), MCPB (pink), and DCPB (blue) by annihilation by stepping between the $E_{\text{p}}^{\text{red}} - 80$ mV and the $E_{\text{p}}^{\text{ox}} + 80$ mV, integration time: 3 min, slit width: 0.75 mm.

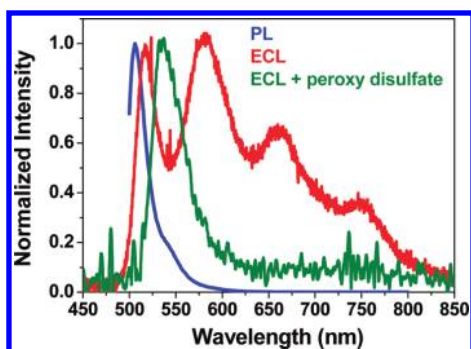


Figure 7. Normalized PL and ECL spectra of PB in MeCN. PL spectrum (blue line, 1 μM PB); ECL spectrum by annihilation (red line, 0.5 mM PB); and ECL spectrum generated with the coreactant peroxydisulfate (green line, 0.5 mM PB with 5 mM peroxydisulfate). ECL spectra were integrated 3 min using a 0.75 mm slit width.

solution concentration used in PL and ECL and by the difference in slit width between the two instruments used for collection of the spectra.²⁰ PL spectra taken by the same CCD camera as for ECL measurements and the same concentration as used for ECL show similar PL wavelength emission in ECL spectra. Thus, in both cases the light is emitted from the same electronically excited state of DCPB. For MCPB, the PL spectrum was also very close to the ECL, however the ECL showed a distinct longer wavelength tail.

The ECL from PB showed multiple emission peaks at longer wavelengths that are not present in the PL spectrum. The first maximum (at 516 nm) was at the same position as the PL peak, that is, emission from the parent singlet excited state. The longer wavelength peaks (at 581, 663, and 752 nm) not seen in the PL spectra are probably due to products from homogeneous reactions of the electrogenerated radical ions, discussed further below. Note that when peroxydisulfate ($\text{S}_2\text{O}_8^{2-}$) was used as a

coreactant to generate ECL only on reduction without preparing radical cations, the longer wavelength peaks were not observed (Figure 7). This suggests the products of the radical cation are contributors, although long wavelength emission could also be from an excimer formed more efficiently in ECL than in PL by the radical ion annihilation. Excimer emission from some BODIPY derivatives in the literature was typically observed between 650 and 670 nm.^{21,22} BODIPY derivatives in a rigid matrix show phosphorescence emission at about 770 nm;^{23,24} it is unlikely however that the ECL emission (at 752 nm) is from the triplet state, which is quenched in the solution phase.

Bulk Electrolysis. Although the fluorescence spectrum of a solution after extensive ECL cycling for 10 min did not show these longer wavelengths and the PL was similar before and after ECL measurements, it is unlikely that sufficient product was formed during these experiments with a small electrode to produce enough long wavelength emitting species in the bulk solution. However, after reductive bulk coulometric electrolysis longer wavelength PL emission was observed. Bulk electrolysis was carried out as described in the Experimental Section in MeCN with 1 mM PB and 0.1 M TBAPF₆ with current–time data recorded during the experiment. The charge passed during 99.5% reduction electrolysis was 0.359 C, which is 92.9% of theoretical charge for a one-electron process (Supporting Information, Figure S8a). In addition, the $i-t$ curve (Supporting Information, Figure S8b) describing the bulk reduction decayed to background in about 15 min. The radical anions produced by the reductive bulk electrolysis were not stable under exposure to oxygen. After a short period of bulk electrolysis at -2.2 V versus Ag/AgNO₃ (MeCN), a deep purple solution was generated from the initial light green colored solution. However, after standing overnight, the solution turned slightly greenish purple. The solution in the first compartment cell was gathered and the chemical ionization mass spectrum and fluorescence spectrum were measured (Supporting Information, Figures S9 and S10).

Chemical ionization mass spectra (CI-MS) of the reduced product of PB after bulk electrolysis were obtained to find products of any reaction of the radical anion (Supporting Information, Figure S9). In the mass spectrum of the reduced solution, three dominant peaks were observed at m/z , 630, 1015.3, and 1789.6. The molecular mass of PB is 638.34 g/mol. The m/z of 1789 can probably be attributed to a protonated trimer form without one iodine atom. This trimer structure may be generated to link through the 2 and 6 positions. The peak at an m/z of 1015.3 corresponds to the dimer missing one iodine atom and one 1-(2-methoxyethoxy) but-2-yl group. This could come from fragmentation of the trimer. Moreover, the PL spectrum of the reduced product of PB after bulk electrolysis showed a peak at a similar longer wavelength as the second peak of the ECL spectrum of PB (Supporting Information, Figure S10). While further studies are needed to elucidate the chemistry of the radical anion, these results suggest a slow loss of iodine followed by following dimerization and trimerization reactions.

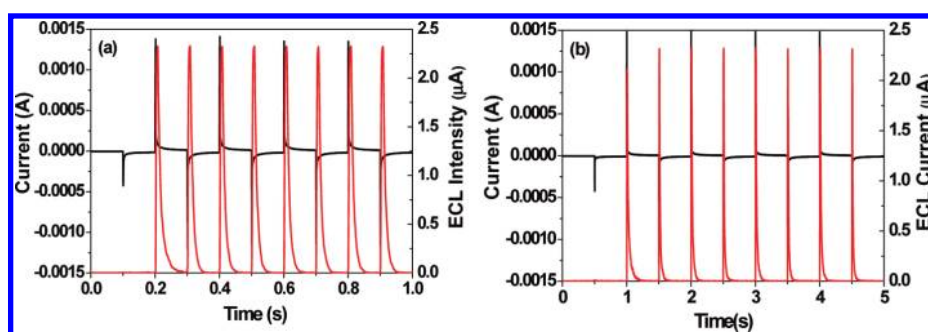


Figure 8. Initial current (black) and ECL light (red) transients for compound DCPB pulsed between +0.84 V and -1.81 V vs SCE. Pulse width is (a) 0.1 and (b) 0.5 s. Conditions as in Figure 6.

ECL Mechanism and Efficiency. The enthalpy of annihilation was estimated from the reversible standard potentials of the redox couples with the equation, $-\Delta H_{\text{ann}} = -\Delta G - T\Delta S = (E_{\text{A}^+/\text{A}}^\circ - E_{\text{A}/\text{A}^-}^\circ) - 0.1 \text{ eV}$.¹¹ This was compared to the energy needed to produce the excited singlet state from the ground state, E_s , to see if the ECL reaction followed the S-route. The enthalpy of annihilation for three BODIPY compounds calculated from the electrochemical data (shown in Table 2) is slightly smaller than the singlet energy from the emission spectra, suggesting the ECL of these BODIPY compounds involves the T-route. However, the relatively intense ECL observed is more consistent with some direct singlet formation, so an ST-route is a possibility.

To estimate the stability of the ECL and the radical ion species, potential pulsing ECL transients were collected. When the potential was stepped from the oxidation wave ($E_{\text{pa}} + 80 \text{ mV}$) to the reduction wave ($E_{\text{pc}} - 80 \text{ mV}$), approximately equal ECL intensities were observed on the anodic and cathodic pulses. For example, DCPB showed symmetrical current pulses and equal ECL emission transients, which show stable behavior with time (Figure 8). Results for PB and MCPB are shown in Supporting Information, Figure S11. The relative ECL quantum yields of these BODIPY compounds are measured in comparison to a widely investigated ECL emitter, 9,10-diphenylanthracene (DPA). These results are given in Table 2. From these measurements, ECL of DCPB is about as strong as DPA under similar conditions.

CONCLUSION

Three new BODIPY compounds were studied. Two of the compounds, with the MCPB and DCPB, give chemically reversible oxidation and reduction in their CV. These new highly fluorescent BODIPY compounds are good candidates for ECL and produce relatively strong ECL emission compared to DPA, a known ECL standard. PB, the least sterically hindered, showed multiple ECL peaks at longer wavelength that is ascribed to instabilities of the PB radical ions. Both the more sterically hindered MCPB and DCPB show good stability of the radical cations, even though the 2 and 6 positions are unsubstituted, probably because the bulky groups on positions 3, 4, and 5 provide some blocking.

ASSOCIATED CONTENT

Supporting Information. Additional simulation information. This material is available free of charge via the Internet at <http://pubs.acs.org>.

AUTHOR INFORMATION

Corresponding Author

*E-mail: ajbard@mail.utexas.edu.

ACKNOWLEDGMENT

We acknowledge support of this research from Roche Diagnostics, Inc., the National Science Foundation (CH-0808927) and the Centre National de la Recherche Scientifique (CNRS).

REFERENCES

- (1) Treibs, A.; Kreuzer, F. H. *Justus Liebig Ann. Chem.* **1968**, 718, 208–223.
- (2) (a) Loudet, A.; Burgess, K. *Chem. Rev.* **2007**, *107*, 4891–4932. (b) Ziessel, R.; Ulrich, G.; Harriman, A. *New J. Chem.* **2007**, *31*, 496–501. (c) Ziessel, R.; Ulrich, G.; Harriman, A. *Angew. Chem., Int. Ed.* **2008**, *47*, 1184–1201.
- (3) (a) Trieflinger, C.; Rohr, H.; Rurack, K.; Daub, J. *Angew. Chem., Int. Ed.* **2005**, *44*, 6943–6947. (b) McCusker, C.; Carroll, J. B.; Rotello, V. M. *Chem. Commun.* **2005**, 996–998. (c) Loudet, A.; Burgess, K. *Chem. Rev.* **2007**, *107*, 4891–4932.
- (4) Brom, J. M.; Langer, J. L. *J. Alloys Compd.* **2002**, *338*, 112–115. (b) Hepp, A.; Ulrich, G.; Schmechl, R.; Von Seggern, H.; Ziessel, R. *Synth. Met.* **2004**, *146*, 11–15.
- (5) (a) Shah, M.; Thangaraj, K.; Soong, M. L.; Wolford, L. T.; Boyer, J. H.; Politzer, I. R.; Pavlopoulos, T. G. *Heteroat. Chem.* **1990**, *1*, 389–399. (b) Sathyamoorthi, G.; Wolford, L. T.; Hagg, A. M.; Boyer, L. H. *Heteroat. Chem.* **1994**, *5*, 245–249. (c) Chen, T.; Boyer, J. H.; Trudell, M. L. *Heteroat. Chem.* **1997**, *8*, 51–54.
- (6) (a) Li, F.; Yang, S. I.; Ciringh, Y.; Seth, J.; Martin, C. H., III; Singh, D. L.; Kim, D.; Birge, R. R.; Bocian, D. F.; Holten, D.; Lindsey, J. S. *J. Am. Chem. Soc.* **1998**, *120*, 10001–10017. (b) Lammi, R. K.; Amboise, A.; Balasubramanian, T.; Wagner, R. W.; Bocian, D. F.; Holten, D.; Lindsey, J. S. *J. Am. Chem. Soc.* **2000**, *122*, 7579–7591. (c) Amboise, A.; Kirmaier, C.; Wagner, R. W.; Loewe, R. S.; Bocian, D. F.; Holten, D.; Lindsey, J. S. *J. Org. Chem.* **2002**, *67*, 3811–3826.
- (7) Hattori, S.; Ohkubo, K.; Urano, Y.; Sunahara, H.; Nagano, T.; Wada, Y.; Tkchanko, N. V.; Lemmetyiene, H.; Fukuzumi, S. *J. Phys. Chem. B* **2005**, *109*, 15368–15375.
- (8) (a) Burghart, A.; Kim, H.; Welch, M. B.; Thoresen, L. H.; Reibenspies, J.; Burgess, K.; Bergstrom, F.; Johansson, L. B.-A. *J. Org. Chem.* **1999**, *64*, 7813–7819. (b) Chen, J.; Burghart, A.; Derecskei-Kovacs, A.; Burgess, K. *J. Org. Chem.* **2000**, *65*, 2900–2906. (c) Beer, G.; Niederalt, C.; Grimme, S.; Daub, J. *Angew. Chem., Int. Ed.* **2000**, *39*, 3252–3255. (d) Rurack, K.; Kollmannsberger, M.; Daub, J. *Angew. Chem., Int. Ed.* **2001**, *40*, 385–387.
- (9) Rebecca, Y. L.; Bard, A. J. *J. Phys. Chem. B* **2003**, *107*, 5036–5042.
- (10) (a) Sunahara, H.; Urano, Y.; Kojima, H.; Nagano, T. *J. Am. Chem. Soc.* **2007**, *129*, 5597–5604. (b) Weidong, C.; Ferrance, J. P.;

- Demas, J.; Landers, J. P. *J. Am. Chem. Soc.* **2006**, *128*, 7572–7578.
- (c) Namba, Y.; Sawada, T.; Suzuki, O. *Anal. Sci.* **2000**, *16* (7), 757–763.
- (11) Bard, A. J., Ed., *Electrogenerated Chemiluminescence*; Marcel Dekker: New York, 2004.
- (12) (a) Faulkner, L. R.; Bard, A. J. In *Electroanalytical Chemistry*; Bard, A. J., Ed.; Dekker: New York, 1977; Vol. 10, pp 1–95. (b) Faulkner, L. R.; Glass, R. S. In *Chemical and Biological Generation of Excited States*; Waldemar, A., Giuseppe, C., Eds.; Academic Press: New York, 1982; Chapter 6. (c) Richter, M. M. *Chem. Rev.* **2004**, *104*, 3003–3036. (d) Knight, A. W.; Greenway, G. M. *Analyst* **1994**, *119*, 879–890. (e) Bard, A. J.; Debad, J. D.; Leland, J. K.; Sigal, G. B.; Wilbur, J. L.; Wohlstadter, J. N. In *Encyclopedia of Analytical Chemistry: Applications, Theory and Instrumentation*; Meyers, R. A., Ed.; John Wiley & Sons: New York, 2000; Vol. 11, p 9842.
- (13) Rousseau, T.; Cravino, A.; Bura, T.; Ulrich, G.; Ziessel, R.; Roncali, J. *Chem. Commun.* **2009**, 1673–1675.
- (14) Sahami, S.; Weaver, M. J. *Electroanal. Chem.* **1981**, *122*, 155–170.
- (15) Burghart, A.; Kim, H.; Wech, M. B.; Thorensen, L. H.; Reibenspies, J.; Burgess, K. *J. Org. Chem.* **1999**, *64*, 7813–7819.
- (16) Nepomnyashchii, A.; Cho, S.; Rossky, P. J.; Bard, A. J. *J. Am. Chem. Soc.* **2010**, *132*, 17550–17559.
- (17) (a) Hoytink, G. J.; van Schooten, J. *Rec. Trav. Chim. Pays-Bas* **1952**, *71*, 1089–1103. (b) Hoytink, G. J.; van Schooten, J. *Rec. Trav. Chim. Pays-Bas* **1953**, *72*, 903–908. (c) Hoytink, G. J.; van Schooten, J.; de Boer, E.; Aalbeersberg, W. I. *Rec. Trav. Chim. Pays-Bas* **1954**, *73*, 355–375. (d) Hoytink, G. J. *Rec. Trav. Chim. Pays-Bas* **1954**, *73*, 895–909.
- (18) Mehlhorn, A.; Schwenzer, B.; Schwetlick, K. *Tetrahedron* **1977**, *33*, 1489–1490.
- (19) Hapiot, P.; Lagrost, C.; Le Floch, F.; Raoult, E.; Rault-Berthelot, J. *Chem. Mater.* **2005**, *17*, 2003–2012.
- (20) Sartin, M. M.; Camerel, F.; Ziessel, R.; Bard, A. J. *J. Phys. Chem. C* **2008**, *112*, 10833–10841.
- (21) Camerel, F.; Bonardi, L.; Schmutz, M.; Ziessel, R. *J. Am. Chem. Soc.* **2006**, *128*, 4548–4549.
- (22) Camerel, F.; Bonardi, L.; Ulrich, G.; Charbonniere, L.; Donnio, B.; Bourgogne, C.; Guillon, D.; Retailleau, P.; Ziessel, R. *Chem. Mater.* **2006**, *18*, 5009–5021.
- (23) Harriman, A.; Rostron, J.; Cesrio, M.; Ulrich, G.; Ziessel, R. *J. Phys. Chem. A* **2006**, *110*, 7994–8002.
- (24) Galletta, M.; Puntoriero, F.; Campagna, S.; Chiorboli, C.; Quesada, M.; Goeb, S.; Ziessel, R. *J. Phys. Chem. A* **2006**, *110*, 4348–4358.